Synthesis, crystal structures, thermal properties, and DNA-binding studies of transition metal complexes with imidazole ligands

Jun Wang [a], Xiangrong Liu [a], Yujin Sun [a], Lanying Yan [a] & Shuiyang He [b]

[a] College of Chemistry and Chemical Engineering, Xi'an University of Science and Technology, Xi'an 710054, P.R. China

[b] College of Chemistry and Materials Science, Northwestern University, Xi'an 710069, P.R. China
Published online: 26 Apr 2011.

PLEASE SCROLL DOWN FOR ARTICLE

Taylor & Francis
Taylor & Francis Group

Synthesis, crystal structures, thermal properties, and DNA-binding studies of transition metal complexes with imidazole ligands

JUN WANG†, XIANGRONG LIU*†, YUJIN SUN†,
LANYING YAN† and SHUIYANG HE‡

†College of Chemistry and Chemical Engineering, Xi'an University of Science and
Technology, Xi'an 710054, P.R. China
‡College of Chemistry and Materials Science, Northwestern University,
Xi'an 710069, P.R. China

A new series of complexes of transition metal (Cu, Zn, Ni) perchlorate with imidazole have been synthesized and characterized by elemental analysis, infrared (IR), UV-Vis spectroscopy, and single-crystal X-ray diffraction. Based on elemental and spectral data, the complexes are $M(C_3H_4N_2)_x(ClO_4)_2$ (M = Cu, Zn, x = 4; M = Ni, x = 6; $C_3H_4N_2$ = imidazole). The crystal structures of $Cu(C_3H_4N_2)_4(ClO_4)_2$ (**1**) and $Zn(C_3H_4N_2)_4(ClO_4)_2$ (**2**) show metals surrounded by four nitrogens of imidazole, while the nickel complex $Ni(C_3H_4N_2)_6(ClO_4)_2$ (**3**) has six nitrogens of imidazole. Intra- and inter-molecular hydrogen bonds exist between hydrogen of imidazole and oxygen of perchlorate. The thermal stabilities of **1**, **2**, and **3** at different heating rates ($\beta = 5°C\,min^{-1}$, $10°C\,min^{-1}$, and $15°C\,min^{-1}$) show that all the complexes exhibit two thermal decomposition stages; the sequence of thermal stability is **2 > 1 > 3**. **1**, **2**, **3**, and imidazole display DNA binding ability, ascertained by UV-Vis titration.

Keywords: Transition metal; Imidazole; Crystal structure; Thermal stability; Interaction with CT-DNA

1. Introduction

Imidazole is one of the most important biological ligands, present in biochemical processes, catalysis, electron transport systems, and nanoparticle electrosynthesis [1, 2]. Transition metal complexes are well suited for application as artificial nucleases because of their cationic nature and diverse 3-D structures depending on the ligand systems. For instance, Zn^{2+} is particularly suited for the construction of coordination compound and networks, as the spherical d^{10} configuration has a flexible coordination environment with geometries varying from tetrahedral to octahedral.

Copper is both vital and toxic for many biological systems [3–5]. Some researchers report that ternary copper(II) complexes have significant cytotoxic activity against the HL-60 cells (myeloid leukemia) and A-549 cells (pulmonary carcinoma) [6], while

---

*Corresponding author. Email: xkchemistry@yahoo.com.cn

another Cu(II) complex is used in DNA-foot-printing experiments, important for detailed study of DNA–protein interactions [7, 8].

Many transition metal complexes bind DNA *via* both covalent and non-covalent interactions. In covalent binding, a labile ligand of the complex is replaced by a nitrogen base of DNA. Non-covalent DNA interactions include intercalative, electrostatic, and groove (surface) binding of cationic metal complexes to the major or minor groove of the DNA helix [9].

Numerous experiments have demonstrated that DNA is the primary intracellular target of anticancer drugs due to the interaction between small molecules and DNA, which can cause DNA damage in cancer cells, blocking the division of cancer cells, and resulting in cell death [10, 11]. Thus, binding of transition metal complexes with DNA is of interest for both therapeutic and scientific reasons and the determinations of these transition metal complex interactions are becoming increasingly important.

Here, we report the synthesis and characterization by elemental analysis, infrared (IR), UV, and single-crystal X-ray diffration of three transition metal perchlorates with imidazole. In order to study the structure–function relationships of the complexes of transition metal perchlorates with imidazole, we investigated their thermal decomposition behaviors and the binding properties with CT-DNA.

2. Experimental

2.1. *Materials*

Imidazole and the transition metallic oxides were of analytical grade and used without purification; the transition metal perchlorates were prepared. CT-DNA was purchased from Sigma Company. CT-DNA was dissolved in *Tris*-HCl buffer ($0.1 \, \text{mol} \, \text{L}^{-1}$, pH $= 7.25$) and its purity checked from the absorbance ratio A_{260}/A_{280}. For all the solutions, this ratio was in the range of 1.8–1.9.

2.2. *Instrumentation*

Melting points were recorded with WBS-1B digital melting point apparatus. Elemental analyses were performed on a P.E.2400 elemental analyzer. IR spectra were recorded on a P.E.983 FT-IR spectrophotometer with a KBr disc from 4000 to $400 \, \text{cm}^{-1}$ and UV-Vis spectra were obtained in CH_3OH at $1.0 \times 10^{-4} \, \text{mol} \, \text{L}^{-1}$ (200–800 nm) by a TU-1900UV-Vis spectrometer.

Thermal data were collected on a Q1000 DSC + LNCS + FACS Q600SDT instrument under nitrogen with heating rates of $5^\circ\text{C} \, \text{min}^{-1}$, $10^\circ\text{C} \, \text{min}^{-1}$, and $15^\circ\text{C} \, \text{min}^{-1}$ from 30°C to 800°C.

X-ray diffraction measurements were performed using a Bruker SMART APEX CCD diffractometer with Mo-Kα radiation ($\lambda = 0.71073 \, \text{Å}$, graphite monochromator). The structures were solved by direct methods and refined by full-matrix least-squares on F^2 with the SHELXL-97 program. Non-hydrogen atoms were located with difference Fourier synthesis and hydrogens were generated geometrically.

Table 1. Physical analytical data for **1–3**.

Complex	Mol. wt	Color	m.p. (°C)	Elemental Anal. Calc. (Found) (%)		
				C	H	N
Cu(C$_3$H$_4$N$_2$)$_4$(ClO$_4$)$_2$ (**1**)	534.76	Dark blue	228–230	26.95(26.89)	3.02(2.87)	20.95(21.63)
Zn(C$_3$H$_4$N$_2$)$_4$(ClO$_4$)$_2$ (**2**)	536.59	White	192–196	26.86(26.93)	3.00(2.50)	20.88(20.74)
Ni(C$_3$H$_4$N$_2$)$_6$(ClO$_4$)$_2$ (**3**)	666.06	Light blue	213–216	32.46(32.85)	3.62(3.52)	25.23(26.59)

2.3. *Preparation of 1–3*

To a methanolic solution (30 mL) of 5 mmol of Cu(II) perchlorate hexahydrate, 20 mmol imidazole was added and the mixture was magnetically stirred at 60°C for 2 h to get clear solution and then filtered and left for a week, after which blue crystals were isolated by filtration. Finally, the crystals were washed with cold ether and dried by concentrated sulfuric acid.

The other transition metal complexes (Zn and Ni) were prepared in a similar way, but the complex of Ni(II) needs 30 mmol imidazole. The complexes have different colors from each other. The physical analytical data for the three complexes are given in table 1.

Caution: Perchlorate salt of metal complex with organic ligand is potentially explosive and should be handled with care.

3. Results and discussion

3.1. *IR spectra*

IR spectra of the complexes showed characteristic bands due to functional groups of imidazole. The important IR spectral bands of the ligand and its metal complexes are given in table 2. The strong band at 3125 cm^{-1} is due to NH of free imidazole [12]. Bands at 1614–1670 and 1535–1547 cm^{-1} can be assigned to C=N and C=C vibrations, respectively. The band at 3306–3383 cm^{-1} belongs to hydrogen bonding (N–H···O). In the far IR region, a medium intensity band at 621–627 cm^{-1} is due to M–N bond vibrations.

Comparing the spectra of the complexes with that of the ligand, the strong bond at 3125 cm^{-1} disappeared, which demonstrates that the ligand coordinates to metal *via* NH group of imidazole and M–N bonds form.

3.2. *UV spectra*

UV spectral data of the ligand and its complexes are listed in table 3. The free ligand exhibits a strong absorption band at 301 nm. The complexes yield new peaks from the ligand. Complexes **1** and **3** have two absorptions. For **1**, the two peaks are centered at

Table 2. Main IR data of imidazole and **1–3** (cm^{-1}).

Compound	$\nu_{N-H\cdots O}$	ν_{C-H}	$\nu_{C=N}$	ν_{N-H}	$\nu_{C=C}$	ν_{O-Cl}	ν_{M-N}
$C_3H_4N_2$	–	3022	1670	3125	1542	–	–
$Cu(C_3H_4N_2)_4(ClO_4)_2$ (**1**)	3306	2947	1614	–	1535	2582	623
$Zn(C_3H_4N_2)_4(ClO_4)_2$ (**2**)	3383	2958	1630	–	1547	2609	621
$Ni(C_3H_4N_2)_6(ClO_4)_2$ (**3**)	3372	2946	1626	–	1538	2626	627

Table 3. UV spectral data of imidazole and **1–3** (nm).

Compound	Absorption	Compound	Absorption
$C_3H_4N_2$	301	$Zn(C_3H_4N_2)_4(ClO_4)_2$ (**2**)	190
$Cu(C_3H_4N_2)_4(ClO_4)_2$ (**1**)	195(395)	$Ni(C_3H_4N_2)_6(ClO_4)_2$ (**3**)	370(605)

195 nm and 395 nm, which are accompanied with a blue-shift of 106 nm and a red-shift of 84 nm up to 301 nm, respectively. For **3**, both at 370 and 605 nm red-shift to 301 nm, showing that complexes have been obtained and different transition metals have different coordination number.

3.3. *Description of the crystal structure*

Details of the crystal structure determinations, including crystal data, data collection, structure determination, and refinement parameters for **1–3**, are summarized in table 4. Selected bond lengths (Å) and angles (°) for **1–3** are listed in table 5. The crystal structures of **1–3** with atomic labeling and the unit cell packing diagrams of **1–3** are shown in figures 1–6, respectively.

X-ray study of **1** reveals that the crystals are monoclinic unit cells, in which each copper is coordinated by four imidazoles. The crystal structure of **1** with the atomic labeling and the unit cell packing diagram are shown in figures 1 and 2, respectively. Imidazole is monodentate. The environment around each copper(II) may be described as tetragon, with ligand–metal–ligand angles varying between N(2)A–Cu(1)–N(3) 90.25(11)° and N(2)–Cu(1)–N(3) 89.75(11)°. The various angles from 90.25(11)° to 89.75(11)° reflect the slight distortion towards planar. The average Cu–N bond distance is similar to those found in other Cu(II) complexes [13–15]. The Cu(1)–N(2) bond distance of 2.005 Å is shorter than Cu(1)–N(3) 2.015 Å, which indicates the steric effect between the ligands. Perchlorate interacts with the complex by charge effect. There are two uncoordinated perchlorates to neutralize the 2+ charge on the Cu(II) complex cation. Finally, the crystal structure is stabilized by a hydrogen-bond network, in which oxygen of perchlorate are acceptors of hydrogen, whereas nitrogen N(3) of imidazole is donors.

The structure of **2** is very similar to that of **1**, with copper(II) substituted by zinc(II), as shown in figures 3 and 4. The Zn–N distance is 1.976(3) or 1.978(3) Å, comparable to that in other imidazole complexes [13, 14]. However, coordination geometry about zinc(II) in **2** is distorted tetrahedral with four nitrogens of imidazole.

Table 4. Crystallographic data and structure refinement parameters.

	1	2	3
Empirical formula	$C_{12}H_{16}Cl_2N_8O_8Cu$	$C_{12}H_{16}Cl_2N_8O_8Zn$	$C_{18}H_{24}Cl_2N_{12}O_8Ni$
Formula weight	534.76	536.59	666.06
Crystal size (mm^3)	$0.31 \times 0.27 \times 0.15$	$0.30 \times 0.21 \times 0.16$	$0.28 \times 0.22 \times 0.13$
Space group	$P2(1)/c$	$C2/c$	$P2(1)/n$
Unit cell dimensions (nm, °)			
a	8.1857(16)	17.945(5)	11.475(2)
b	16.350(3)	7.022(2)	7.2071(14)
c	8.0614(16)	19.748(8)	16.223(3)
β	109.783(3)	116.328(5)	90.036(3)
Volume (nm^3), Z	1015.2(3), 2	2230.4(13), 4	1341.7(5), 2
Calculated density ($Mg\,m^{-3}$)	1.736	1.598	1.634
Absorption coefficient (mm^{-1})	1.398	1.395	0.990
$F(000)$	534	1088	672
θ range (°)	2.49–25.10	2.30–25.09	2.17–25.09
Reflections collected	4964	5381	6395
Independent reflections	1810 [R(int) $= 0.0321$]	1995 [R(int) $= 0.0368$]	2378 [R(int) $= 0.0455$]
Goodness-of-fit on F^2	1.014	1.036	1.093
Final R indices [$I > 2\sigma\,(I)$]	$R_1 = 0.0501$, $\omega R_2 = 0.1324$	$R_1 = 0.0503$, $\omega R_2 = 0.1199$	$R_1 = 0.0498$, $\omega R_2 = 0.1454$
R indices (all data)	$R_1 = 0.0588$, $\omega R_2 = 0.1361$	$R_1 = 0.0762$, $\omega R_2 = 0.1288$	$R_1 = 0.0629$, $\omega R_2 = 0.1640$
Largest difference peak and hole (e nm^{-3})	0.568 and -0.982	0.320 and -0.559	0.583 and -0.486

Table 5. Selected bond lengths (Å) and angles (°) for **1–3**.

1		**3**	
Cu(1)–N(2)A	2.005(3)	Ni(1)–N(3)A	2.127(3)
Cu(1)–N(2)	2.005(3)	Ni(1)–N(3)	2.127(3)
Cu(1)–N(3)A	2.015(3)	Ni(1)–N(1)	2.135(3)
Cu(1)–N(3)	2.015(3)	Ni(1)–N(1)A	2.135(3)
N(2)A–Cu(1)–N(2)	180.0	Ni(1)–N(5)	2.141(3)
N(2)A–Cu(1)–N(3)A	90.25(11)	Ni(1)–N(5)A	2.141(3)
N(2)–Cu(1)–N(3)A	89.75(11)	N(3)A–Ni(1)–N(3)	180.0
N(2)A–Cu(1)–N(3)	89.75(11)	N(3)A–Ni(1)–N(1)	88.46(12)
N(2)–Cu(1)–N(3)	90.25(11)	N(3)–Ni(1)–N(1)	91.54(12)
N(3)A–Cu(1)–N(3)	180.0	N(3)A–Ni(1)–N(1)A	91.54(12)
		N(3)–Ni(1)–N(1)A	88.46(12)
2		N(1)–Ni(1)–N(1)A	180.0
Zn(1)–N(1)A	1.976(3)	N(3)A–Ni(1)–N(5)	89.43(12)
Zn(1)–N(1)	1.976(3)	N(3)–Ni(1)–N(5)	90.57(12)
Zn(1)–N(2)	1.978(3)	N(1)–Ni(1)–N(5)	91.14(12)
Zn(1)–N(2)A	1.978(3)	N(1)A–Ni(1)–N(5)	88.86(12)
N(1)A–Zn(1)–N(1)	105.4(2)	N(3)A–Ni(1)–N(5)A	90.57(12)
N(1)A–Zn(1)–N(2)	108.23(13)	N(3)–Ni(1)–N(5)A	89.43(12)
N(1)–Zn(1)–N(2)	111.13(14)	N(1)–Ni(1)–N(5)A	88.86(12)
N(1)A–Zn(1)–N(2)A	111.13(14)	N(1)A–Ni(1)–N(5)A	91.14(12)
N(1)–Zn(1)–N(2)A	108.23(13)	N(5)–Ni(1)–N(5)A	180.0
N(2)–Zn(1)–N(2)A	112.53(19)		

In order to describe four-coordinate transition metal complexes, the τ parameter introduced by Houser [16] is used to assess molecular shape. The τ parameter can be calculated by equation (1).

$$\tau = \frac{360° - (\alpha + \beta)}{141°} \tag{1}$$

Figure 1.   Perspective view with atom labeling of **1**.

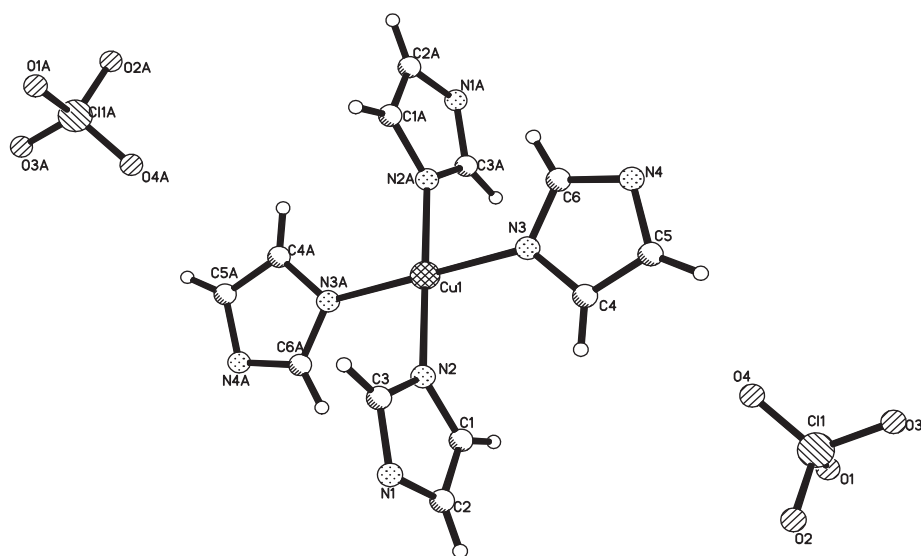Figure 2.   Packing diagram of **1** in a cell.

J. Wang et al.

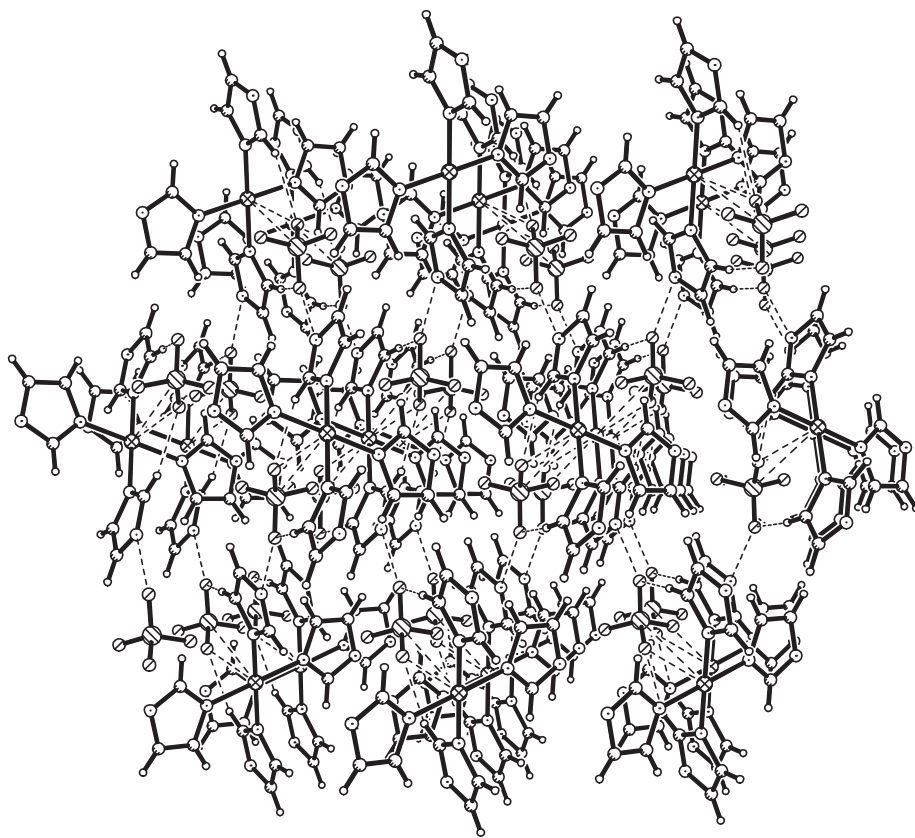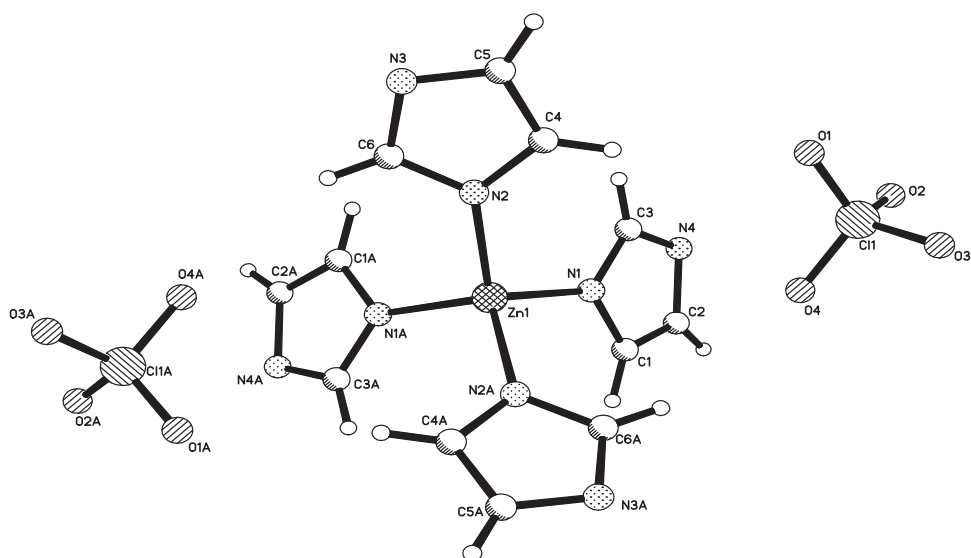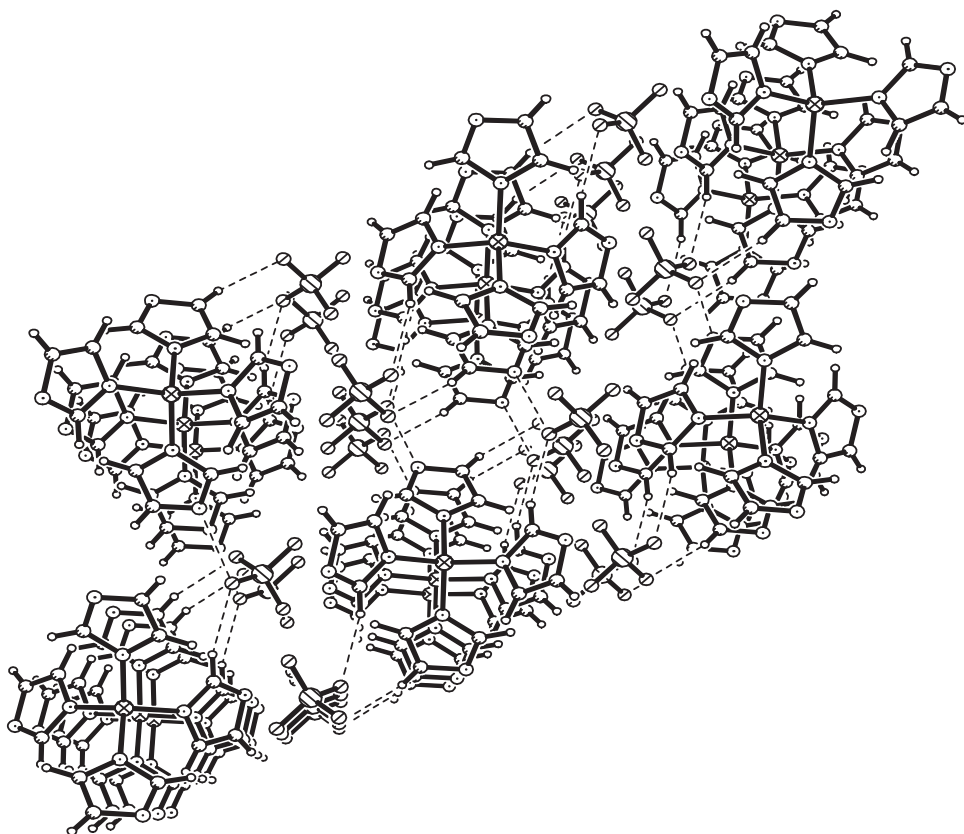Figure 3.   Perspective view with atom labeling of **2**.

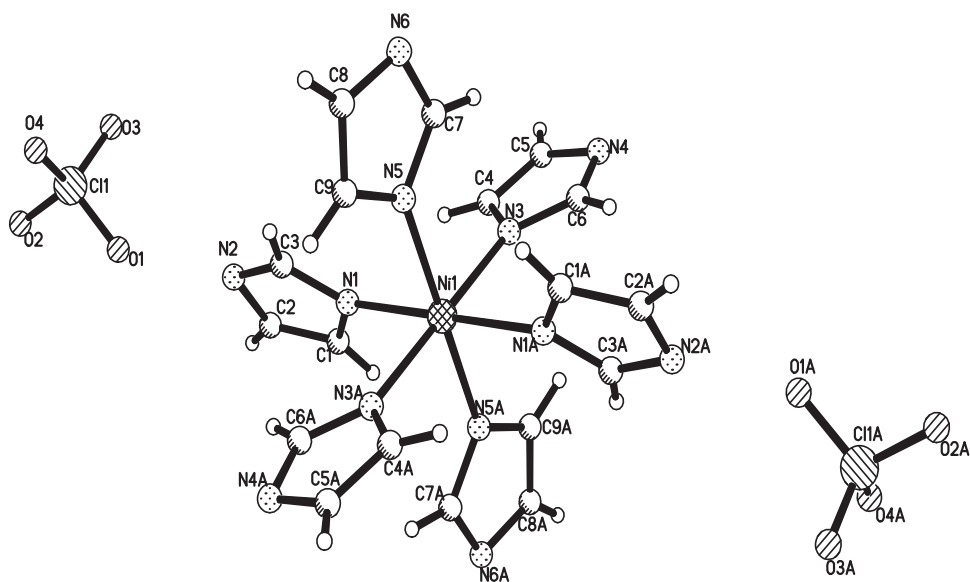Figure 4.   Packing diagram of **2** in a cell.

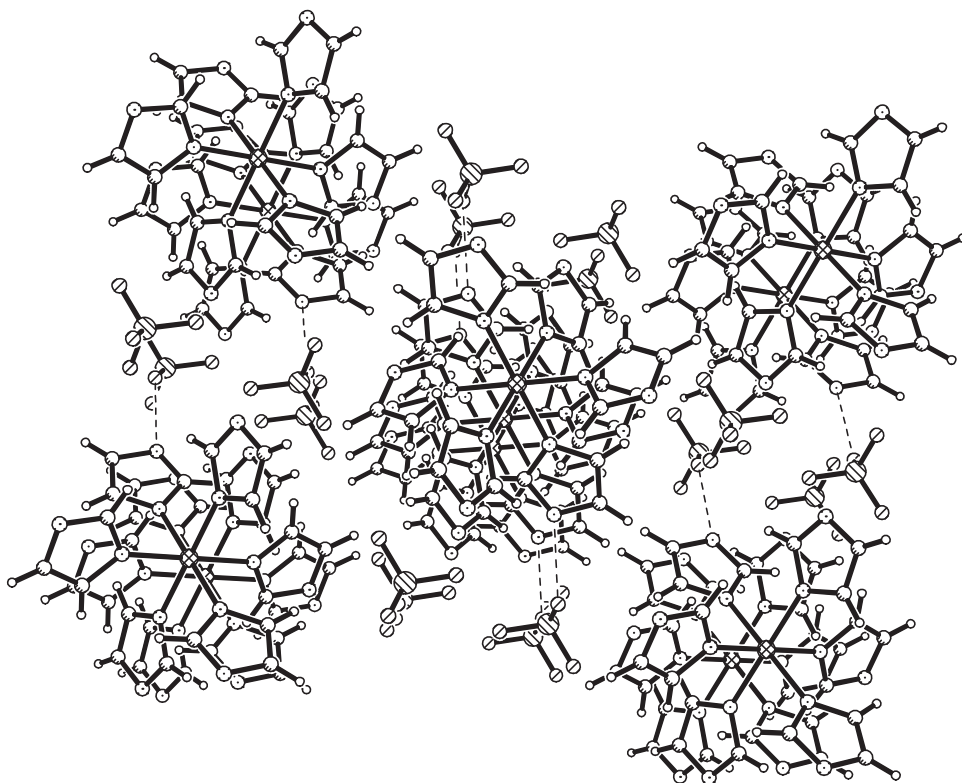Figure 5. Perspective view with atom labeling of **3**.

Figure 6. Packing diagram of **3** in a cell.

Values of τ range from 1.00 for a perfect tetrahedral geometry to zero for a perfect square planar geometry. The τ parameter of **2** is 0.97, indicating a slightly distorted tetrahedral geometry.

Complex **3** also belongs to monoclinic crystal; the structure with atomic labeling and the unit cell packing diagram are shown in figures 5 and 6. The environment around nickel(II), which is coordinated by six imidazoles, may be described as a slightly distorted octahedral geometry with ligand–metal–ligand angles varying between N(3)A–Ni(1)–N(1)A 91.54° and N(3)–Ni(1)–N(5)A 89.43°. The average Ni–N bond distance is 2.134 Å, which is similar to those found in other Ni(II) complexes [14, 17]. The crystal structure is stabilized by a O$\cdots$H(1)–N(1) intermolecular bond. The hydrogen bonding interaction of **3** is similar to **1** and **2**. The N–C bond varies owing to combination of imidazole with nickel(II), but the ring skeleton of imidazole has not changed. The mean value M–N bond lengths are 2.010 Å, 1.977 Å, and 2.134 Å for **1**, **2**, and **3**, respectively, which means zinc(II) has better coordination ability to imidazole than copper(II) and nickel(II).

3.4. Thermal analysis

Thermal gravimetric (TG) and differential thermogravimetry (DTG) of **1**–**3** were carried out between 30°C and 800°C at 5°C min^{-1}, 10°C min^{-1}, and 15°C min^{-1}. "Supplementary material" shows the TG–DTG curves recorded in nitrogen at 15°C min^{-1}; the TG–DTG curves at 5°C min^{-1} and 10°C min^{-1} are similar with these.

Complex **1** is stable to 228°C at which it begins to melt. The TG–DTG curves of **1** indicate the release of four imidazoles from 251°C to 400°C (observed 51.62%, Calcd 50.09%) to give $Cu(ClO_4)_2$. Decomposition of perchlorate takes place at 495–730°C and the experimental mass loss of 31.44% is consistent with the calculated value of 34.20% for elimination of two ClO_3. The solid residue formed at 620°C is suggested to be CuO (observed 16.94%, Calcd 14.88%) [18].

Complexes of Zn(II) and Ni(II) decompose in two steps, similar to thermal decomposition of **1**. However, there are several differences among these complexes.

Complex **2** is stable to 234°C at which it begins to decompose. The TG–DTG curves of **2** releases three imidazoles and one perchlorate between 223–425°C (observed 58.58%, Calcd 56.60%). The solid residue formed at 342°C is $Zn(C_3H_4N_2)(ClO_4)$ [19]. The weight loss of 27.83% from 443°C to 774°C is equivalent to the loss of one imidazole and one ClO_3 (Calcd 28.23%). The solid residue formed at 600°C is ZnO (observed 13.49%, Calcd 15.16%).

Complex **3** is stable to 202°C at which it begins to melt. The TG–DTG curves of **3** indicate the release of six imidazoles at 325°C (observed 61.02%, Calcd 61.32%) to give $Ni(ClO_4)_2$, which is stable to 445°C. Decomposing of the perchlorate takes place from 450–760°C and the experimental mass loss of 21.58% is consistent with the calculated value of 19.22% for the elimination of gaseous oxygen. The solid residue formed at 620°C is suggested to be $NiCl_2$ (observed 17.49%, Calcd 19.45%). Similar decomposition behavior has been observed [20–22].

In section 3.3, we observed that the order of M–N binding is **2** > **1** > **3**. Comparison of TG and DTG curves of **1**–**3** under identical experimental conditions ($\beta = 15$°C min^{-1}) shows that the stability of the complexes decreases in the same order: $Zn(C_3H_4N_2)_4(ClO_4)_2$ > $Cu(C_3H_4N_2)_4(ClO_4)_2$ > $Ni(C_3H_4N_2)_6(ClO_4)_2$ [23].

3.5. *DNA binding study*

Before adding CT-DNA to **1**, **2**, and **3**, their behaviors in buffer solution at room temperature were monitored by UV–Vis spectroscopy. Liberation of imidazole was not observed, suggesting that the complexes are stable under the conditions.

The binding of **1–3** to DNA helix has been characterized through absorption spectral titrations by following changes in absorbance and shift in wavelength. Figure 7 shows absorption spectra of copper(II), zinc(II), and nickel(II) complexes in the presence of CT-DNA. Addition of increasing amounts of CT-DNA results in hyperchromism and a small shift.

Upon addition of CT-DNA, absorptions of **1**, **2**, **3**, and imidazole at 258 nm show hyperchromism, and are accompanied by a small shift in λ_{max}, from 257 to 259 nm of **2** and no shift for **1**, **3**, and imidazole. The hyperchromicity indicates that the binding of these complexes as 1.0×10^{-5} mol L^{-1} solutions towards CT-DNA should not be intercalation, since intercalation leads to hypochromism in spectra due to strong stacking interactions between the complex and the base pairs of DNA [11, 24]; Gao *et al.* [25] have found zinc(II) and nickel(II) complexes with CT-DNA have hypochromism from intercalation, different from the interactions of **1–3** with CT-DNA.

As the DNA double helix possesses many hydrogen-bonding sites, it is likely that those complexes bearing N–H form hydrogen bonds with DNA, which is consistent with groove binding. This hyperchromism can be attributed either to external contact (surface binding) with the duplex or to the fact that the complexes could uncoil the helix structure of DNA and make more bases in DNA exposed. Some similar hyperchromism, such as Cu(II) complex with N–H of the amino acid, have been observed [6, 11, 26].

Among the factors governing the binding modes, the most significant is molecular shape [27]; the significant difference in DNA-binding affinity of the three complexes can result from different molecular geometry. Complex **1** is nearly planar with less steric effect than **2** and **3**, increasing the binding ability of Cu(II) complex with DNA. Interaction of **2** with DNA is stronger than **3** for similar reasons. Comparison of the absorption spectra of **1**, **2**, and **3** under identical experimental conditions ($\gamma = $ [complex]/[DNA] = 1/3), in figure 8, indicates that the binding strength of those complexes is $Cu(C_3H_4N_2)_4(ClO_4)_2 > Zn(C_3H_4N_2)_4(ClO_4)_2 > Ni(C_3H_4N_2)_6(ClO_4)_2$; a similar hyperchromism has been found in the literature [26].

4. Conclusion

We prepared and characterized a series of complexes of Cu, Zn, Ni perchlorate with imidazole and the crystal structures of **1**, **2**, and **3** were determined. The environment around copper(II), zinc(II), and nickel(II) may be described as tetragon, slightly distorted tetrahedral and slightly distorted octahedral, respectively. The crystal structure is stabilized by a hydrogen-bond network, in which oxygens of perchlorate are acceptors of hydrogen and nitrogen of imidazole donors. The thermal stability of the complexes is **2** > **1** > **3**. Interactions of imidazole and the complexes with CT-DNA
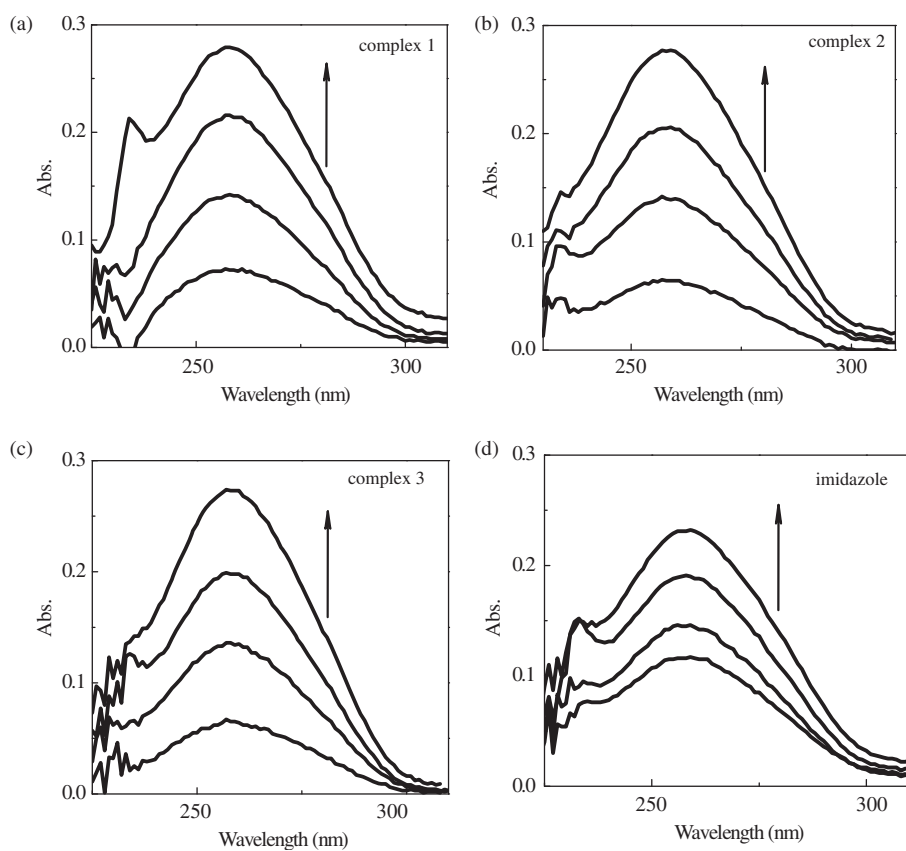
Figure 7. Absorption spectra of 1.0×10^{-5} mol L^{-1} **1** (a), **2** (b), **3** (c), and imidazole (d) in the presence of CT-DNA at increasing amounts. The arrows show the changes upon increasing amounts of CT-DNA.
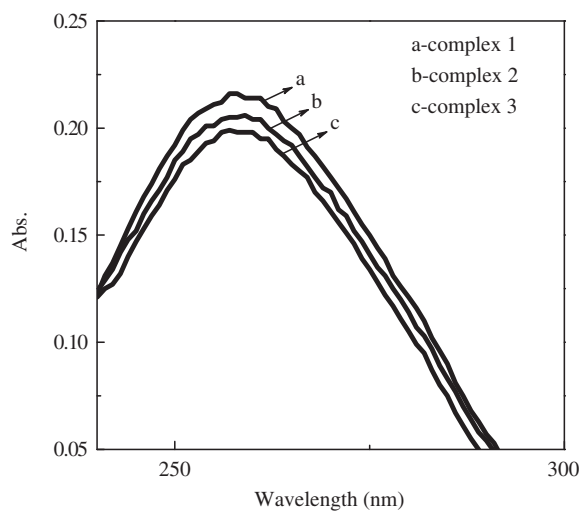

Figure 8. The absorption spectra of **1**(a), **2**(b), and **3**(c) under identical experimental conditions ($\gamma =$ [complex]/[DNA] $= 1/3$).

have been studied with UV spectroscopy revealing their ability to bind to DNA mainly by groove binding or surface binding with the duplex of DNA.

Supplementary material

Acknowledgments

References

[1] R.N. Patel, V.L.N. Nripendra Singh, R.N. Gundla. *Polyhedron*, **25**, 3312 (2006).
[2] R.N. Patel, V.L.N. Gundla, D.K. Patel. *Polyhedron*, **27**, 1057 (2008).
[3] B. Dede, F. Karipcin, M. Cengiz. *J. Hazard. Mater.*, **163**, 1149 (2009).
[4] Z.L. Chen, J. Miao, Z. Zhang, F.P. Liang, Q. Wu. *J. Organomet. Chem.*, **695**, 193 (2010).
[5] W. Zhao, J. Fan, T. Okamura, W.Y. Sun, N. Ueyama. *Microporous Mesoporous Mater.*, **78**, 270 (2005).
[6] L. Jia, P. Jiang, J. Xu, Z.Y. Hao, X.M. Xu, L.H. Chen, J.C. Wu, N. Tang, Q. Wang, J.J. Vittal. *Inorg. Chim. Acta*, **363**, 857 (2010).
[7] W.K. Pogozelski, T.D. Tullius. *Chem. Rev.*, **98**, 1089 (1998).
[8] S.A. Pati, V.H. Naik, A.D. Kulkarni, U. Kamble, G.B. Bagihalli, P.S. Badami. *J. Coord. Chem.*, **63**, 688 (2010).
[9] Z.H. Xu, F.J. Chen, P.X. Xi, X.H. Liu, Z.Z. Zeng. *J. Photochem. Photobiol., A: Chemistry*, **196**, 80 (2008).
[10] C. Hemmert, M. Pitié, M. Renz, H. Gornitzka, S. Soulet, B. Meunier. *J. Biol. Inorg. Chem.*, **6**, 14 (2001).
[11] G. Zuber, J.C. Quada Jr, S.M. Hecht. *J. Am. Chem. Soc.*, **120**, 9368 (1998).
[12] M. Arif, Nazir, M.S. Iqbal, S. Anjum. *Inorg. Chim. Acta*, **362**, 1626 (2009).
[13] A. Dołega, A. Farmas, K. Baranowska, A. Herman. *Inorg. Chem. Commun.*, **12**, 825 (2009).
[14] G. Brewer, C. Brewer, R.J. Butche, E.E. Carpenter. *Inorg. Chim. Acta*, **359**, 1265 (2006).
[15] S.G. Baca, M.T. Reetz, R. Goddard, I.G. Filippova, Y.A. Simonov, M. Gdaniec, N. Gerbeleu. *Polyhedron*, **25**, 1217 (2006).
[16] L. Yang, D.R. Powell, R.P. Houser. *J. Chem. Soc., Dalton Trans.*, 955 (2007).
[17] D.K. Patel, D. Choquesillo-Lazarte, J.M. González-Pérez, A. Domínguez-Martín, A. Matilla-Hernandez, A. Castiñiras, J. Niclós-Gutiérrez. *Polyhedron*, **29**, 686 (2010).
[18] G. Singh, S.P. Felix, D.K. Pandey. *Thermochim. Acta*, **411**, 69 (2004).
[19] M.G. Amiri, A. Morsali, A.D. Hunter, M. Zeller. *Solid State Sci.*, **9**, 1081 (2007).
[20] Y.Y. Di, Z.C. Tan, Y.S. Li. *Acta Chim. Sinica*, **13**, 1396 (2006).
[21] X.Y. Li, Y.H. Yang. *Acta Chim. Sinica*, **53**, 583 (1995).
[22] W.W. Yang, Y.Y. Qiu, Y.X. Kong, Z.C. Tan. *Chin. J. Inorg. Chem.*, **26**, 1252 (2010).
[23] G. Singh, C.P. Singh, S.M. Mannan. *Thermochim. Acta*, **437**, 23 (2005).
[24] X.Y. Liu. *J. Beijing Union Univ. (Natural Sci.)*, **23**, 20 (2009).
[25] C.Y. Gao, X.F. Ma, J.L. Tian, D.D. Li, S.P. Yan. *J. Coord. Chem.*, **63**, 115 (2010).
[26] A. Tarushi, G. Psomas, C.P. Raptopoulou, V. Psycharis, D.P. Kessissoglou. *Polyhedron*, **28**, 3275 (2009).
[27] N. Raman, R. Jeyamurugan, R. Usha Rani, T. Baskaran, L. Mitu. *J. Coord. Chem.*, **63**, 1629 (2010).